

**INTERNATIONAL JOURNAL OF CURRENT RESEARCH IN  
CHEMISTRY AND PHARMACEUTICAL SCIENCES**

(p-ISSN: 2348-5213; e-ISSN: 2348-5221)

[www.ijcrpcs.com](http://www.ijcrpcs.com)

DOI: 10.22192/ijcrpcs

Coden: IJCROO(USA)

Volume 6, Issue 12 - 2019

**Research Article**



DOI: <http://dx.doi.org/10.22192/ijcrpcs.2019.06.12.001>

**Study of iron (III) hydroxide precipitation in bicarbonate aqueous solutions**

**Wided Mejri<sup>a</sup>, Abdou Salam Manzola<sup>b\*</sup>, Mohamed Tlili<sup>ac</sup> and  
Mohamed Ben Amor<sup>a</sup>**

<sup>a</sup> Natural Water Treatment Laboratory, Water Researches and Technologies Center (CERTE), Technopark of Borj-Cedria, p/o box 273, Soliman 8020, Tunisia.

<sup>b</sup> Laboratory of analytical chemistry and mineral, Faculty of Science and Technology, Abdou Moumouni University BP 10662. Niamey, Niger

<sup>c</sup> Department of Chemistry, College of Sciences – King Khalid University, 9033 Abha, Saudi Arabia

\*Corresponding author: [abdoussalam\\_manzola@yahoo.com](mailto:abdoussalam_manzola@yahoo.com)

**Abstract**

The iron hydroxide Fe(OH)<sub>3</sub> precipitation in bicarbonate aqueous solutions from ferrous sulfate solutions was investigated. Precipitation method consists of the oxidation of Fe(II) by aeration then precipitation of Fe(OH)<sub>3</sub>. The effect of initial pH (pHi) (6-8), HCO<sub>3</sub><sup>-</sup> concentration (1-8 mM) and temperature (20-60 °C) were studied. At a pHi over 6.8, total of iron was precipitate in less than 8 minutes because the autocatalytic effect of iron (III) hydroxide particles on iron (II) oxidation reaction. Bicarbonate concentration increasing was promoted massive Fe(OH)<sub>3</sub> precipitation and was increased precipitation ratio due to the formation of an iron (II)-bicarbonate complex and the buffering effects of bicarbonate ions. At high temperature fast and massive Fe(OH)<sub>3</sub> precipitation were occurred. At 20°C, a complete Fe(OH)<sub>3</sub> precipitation was required 150 min, when it was required just 10 min at 60°C. The X-ray diffraction and FTIR analysis were provided that Fe(OH)<sub>3</sub> precipitation was lead to a sequential formation of lepidocrocite. The pH or temperature increasing was promoted the formation of amorphous iron (III) oxyhydroxyde.

**Keywords:** Iron (III) precipitation, oxidation, Fe(OH)<sub>3</sub>, pH, bicarbonate, temperature, characterization

**INTRODUCTION**

One of the most significant problems in using groundwater for water supply is Fe(II) content. Because of the reducing conditions in groundwater, the concentration of Fe(II) in groundwater is usually in the range of 3-4 mg/L and in some cases up to 10 mg/L<sup>1,2</sup>. When present, even at low concentrations, it causes various aesthetic and operational problems, including bad taste, rust color, support the development of ferrobacteria<sup>3,4</sup>. Once groundwater exposed to air, Fe(II) oxidizes and precipitates to Fe(OH)<sub>3</sub>. Several techniques were developed for iron treatment. The most commonly used was oxidation by

air, followed by precipitation and filtration system<sup>3,5,6</sup>. The iron removal efficiency depends on the kinetics of Fe(II) oxidation and Fe(OH)<sub>3</sub> precipitation. Oxidation and precipitation of Fe(II) are a complex process involving a sequence of steps, including oxidation, hydrolysis, polymerization and precipitation (nucleation and crystal growth). The rate of each step depends on pH, water composition and temperature<sup>7,8,9</sup>. Several authors have studied the effect of pH on Fe(II) oxidation and precipitation rate in aqueous solutions<sup>10,11,12,13,14</sup>. According to (Stumm, 1956)<sup>8</sup>, the kinetically limiting step for iron precipitation using aeration method at pH around 7 is the oxidation rate.

The authors described that the rate of Fe(II) oxidation increases by a first-order kinetic model, and estimated rate constants as 3.7, 7.9 and 12.3 h<sup>-1</sup> at pH 8.4, 8.7 and 9.0, respectively. On the other hand, (Grundl et al., 1993)<sup>15</sup>, studied the iron precipitation in aqueous solutions and found that the kinetics of precipitation at low pH is described by an initial slow nucleation rate followed by a more rapid rate of crystallite growth. The precipitation of the ferric solid form Fe(OH)<sub>3(aq)</sub> was found to be the rate controlling step. Moreover, for more alkaline pH, the reaction is even faster, but the dominant pathway shifts from homogeneous to heterogeneous because Fe(OH)<sub>3(aq)</sub> rapidly precipitates to Fe(OH)<sub>3(s)</sub><sup>10,16</sup>. The effect of pH on the oxidation of Fe(II) is attributed to the hydrolysis species having different oxidation rate<sup>17,18,19</sup>. Fe(OH)<sub>3</sub> precipitation kinetics is also influenced by groundwater composition mainly bicarbonate. Bicarbonate has been reported to have a catalytic effect on Fe(OH)<sub>3</sub> precipitation<sup>20,21</sup>. (King et al., 1995)<sup>14</sup> developed a mixed specific interaction-ion-pairing model for Fe(II) speciation and oxidation by molecular oxygen as a function of pH and media composition. The model determines that ferrous carbonate complexes (FeCO<sub>3</sub>, Fe(CO<sub>3</sub>)<sup>2-</sup>, Fe(CO<sub>3</sub>)OH<sup>-</sup>) dominate the speciation of Fe(II) in natural waters containing greater than 1 mM carbonate alkalinity. (Millero and Izaguirre, 1990)<sup>22</sup> have studied the effects of carbonate on Fe(II) oxidation in a solution containing 0.7 mol/kg of NaCl. They show that the rates of oxidation are increased with added carbonate. This is in agreement with (Ghosh, 1962)<sup>11</sup>. This suggests that the formation of carbonate ion pairs is also important (Fe(HCO<sub>3</sub>)<sup>+</sup>, Fe(CO<sub>3</sub>)<sup>23,25</sup>). The effect of temperature in the studied range (20–60°C) on Fe(OH)<sub>3</sub> precipitation kinetics was less studied. Only a few results are reported in the literature<sup>13,14</sup>. They show that Fe(OH)<sub>3</sub> precipitation rate increases with temperature. (Sung and Morgan, 1992)<sup>12</sup>, report the increasing of the rate when temperature raising by 15 °C. The pH, the water composition and temperature despite influencing the Fe(OH)<sub>3</sub> precipitation kinetics also influence the crystal structure of the final precipitates phase<sup>25,26,27</sup>. In fact, the properties of the final precipitate product are related to the conditions under which they are formed<sup>28,29</sup>. For example, a faster oxidation rates lead to higher intermediate concentrations of dissolved Fe(III), which promotes nucleation of more soluble and less stable poorly crystalline precipitates, such as ferrihydrite (Fe<sub>5</sub>HO<sub>8</sub>.4H<sub>2</sub>O)<sup>7</sup>. Hence, slow oxidation favors the growth of crystalline oxides. In natural water conditions, the eventual products of iron (III) precipitation process is generally a lepidocrocite (-FeOOH)<sup>13,27,30,31</sup>. (Gu and Hsu, 1987)<sup>32</sup> are studied the effect of Fe(OH)<sub>3</sub> precipitation rate on the physical characteristics of the final iron precipitates. They show that precipitation rates were controlled by pH and temperature solution. When the rate was rapid, all the

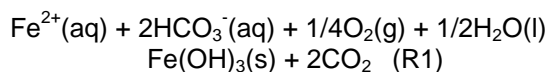
Fe(III) ions precipitate instantaneously to Fe(III) oxides. The obtained particles are very fine, redissolve easily, and subsequently recrystallize to goethite (-FeOOH) or hematite (-Fe<sub>2</sub>O<sub>3</sub>) or both. When the rate was slow, iron(III) ions form nuclei first, followed by crystal growth via deposition of monomeric species on the nuclei. However, despite the considerable amount of research performed to elucidate iron hydroxide precipitation mechanism in relation to water treatment and to probe the effects of some parameters on its kinetic parameters, there is not yet a full understanding of the overall processes of iron (III) precipitation. Thus, a good comprehension of Fe(OH)<sub>3</sub> precipitation, crystallization and the estimation of the effect of pH, temperature and bicarbonate concentration on iron (III) precipitation kinetics seems indispensable.

The focus of this study is to develop a deeper understanding of iron (III) hydroxide precipitation mechanisms and to examine the effect of pH, bicarbonate ions concentration and temperature on iron (III) precipitation kinetics and on the crystal structure of precipitate. We investigated the precipitation of Fe(OH)<sub>3</sub> in bicarbonate aqueous solutions by the degassing method to simulate conditions encountered in natural waters. The Fe(II) ions concentration, dissolved oxygen, pH and temperature were recorded. The obtained precipitates were identified by recording X-ray diffraction and Fourier-transform infrared spectroscopy.

## MATERIALS AND METHODS

### Work solutions

In our study for precipitation deferrization, we used an assembly consisting of an open glass flask of 1L, containing studying solution. The flask was immersed in a controlled temperature bath. All manipulations were carried out in this open glass flask of 1L at atmospheric pressure and initial Fe(II) concentration [Fe(II)]<sub>0</sub> = 25 mg/L in order to increase the contact between the oxygen in the air and the Fe(II) ions in the solution, which is the driving principle behind the evolution of the system leading to the oxidation of the Fe(II) ions and the precipitation of Fe(OH)<sub>3</sub>. The bicarbonated water was prepared by dissolving varying amounts of NaHCO<sub>3</sub> in distilled water. Agitation introduces atmospheric oxygen into the solution. The contact of the solution with atmospheric air causes the release of dissolved CO<sub>2</sub>, which leads to alkalization of the medium, resulting in an increase in pH. This increase in pH was favoured the oxidation of Fe(II) to Fe(III) and the precipitation of Fe(OH)<sub>3</sub><sup>12</sup>. The overall precipitation response was as follows:



The iron hydroxide obtained according to the R1 reaction was very unstable, which explains its evolution towards another iron oxyhydroxide more thermodynamically stable, it was lepidocrocite in its non-hydrated form according to the following reaction:



Several series of tests were performed by varying: the concentration of bicarbonate, the initial pH (pHi) and the temperature. Iron solution was prepared by introducing 99.28 mg of  $\text{FeSO}_4 \cdot 7\text{H}_2\text{O}$  iron sulfate heptahydrate into bicarbonated water to reach  $[\text{Fe}(\text{II})]_0 = 25 \text{ mg/L}$ . The initial pH values were determined by stripping  $\text{CO}_2$  into the bicarbonated water. The effect of bicarbonate concentration, initial pH and temperature were studied.

### Experimental set-up

The experimental set-up used for  $\text{Fe}(\text{OH})_3$  precipitation is shown in Figure 1. In order to initiate iron precipitation, the solution was aerated by a continuous stirring (500 rpm). The period of precipitation test was fixed at 200 min. To determine the concentration of iron in solution

during the precipitation experiment, 1 ml samples were taken using a 5 ml syringe with a  $0.45 \mu\text{m}$  membrane filtration system and immediately added to 1 mL of chlorhydric acid solution (0.1M). Samples of 1mL were taken every 2 minutes, then every 10 minutes of precipitation. The determination of total iron concentration was carried out by using 1-10 phenanthroline method. The samples were analyzed by spectrophotometer (UV/VIS, V-530 JASCO). The pH and temperature, were measured respectively, by a digital Hanna pH-meter (Hanna 221) and a probe temperature were continuously recorded. A dissolved oxygen sensor (CellOx 325) was used to check the oxygen concentration.

The obtained solids were filtered through a  $0.45 \mu\text{m}$  filter, then characterized by x-ray diffraction (XRD) and infrared spectroscopy. Fourier Transform Infrared spectroscopy (FTIR) spectra were recorded with IRAfinity-1 FTIR spectrophotometer with KBr pellet technique at wave numbers of 4000 to  $400 \text{ cm}^{-1}$ . XRD was carried out at room temperature with a Philips X' PERT PRO diffractometer in step scanning mode using  $\text{Cu}_K$  radiation. The XRD patterns were recorded in the scanning range  $2\theta = 15 - 60^\circ$ . A small angular step of  $2\theta = 0.017^\circ$  and a fixed counting time of 4 s were used.

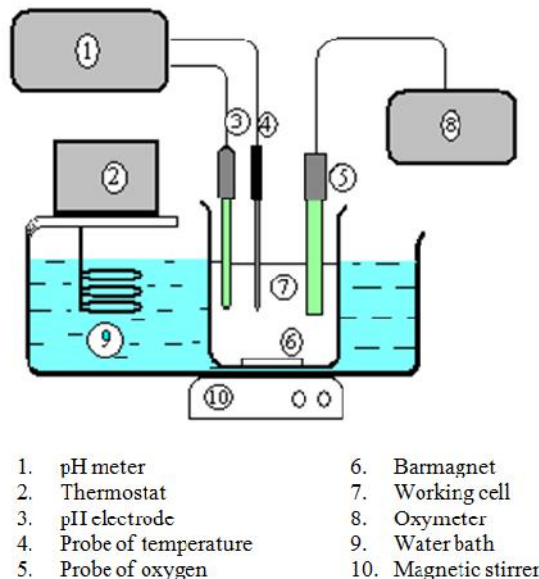


Figure 1: Experimental set-up for iron (III) precipitation test

## RESULTS AND DISCUSSION

### Iron (III) precipitation in Fe(II)-Fe(III)-HCO<sub>3</sub><sup>-</sup>-CO<sub>2</sub>-O<sub>2</sub>-H<sub>2</sub>O- Fe(OH)<sub>3</sub> system

Figure 2 presents pH, dissolved oxygen concentration and total iron concentration with time during Fe(OH)<sub>3</sub> precipitation. During the first 70 minutes, the pH was increased from 6 to 6.35, the dissolved oxygen

concentration was increased from 3 to 6.37 mg/L and the total iron concentration was decreased from 25 to 21 mg/L. The increase of pH is due to the release of CO<sub>2</sub> (reaction 2) and the consumption of H<sup>+</sup> (reaction 3). The increase in the dissolved O<sub>2</sub> causes spontaneous Fe(II) oxidation (reaction 3) followed by Fe(OH)<sub>3</sub> precipitation with a slow precipitation rate (reaction 4)<sup>17</sup>. Reactions 3 and 4 are successive and no discernible steps.

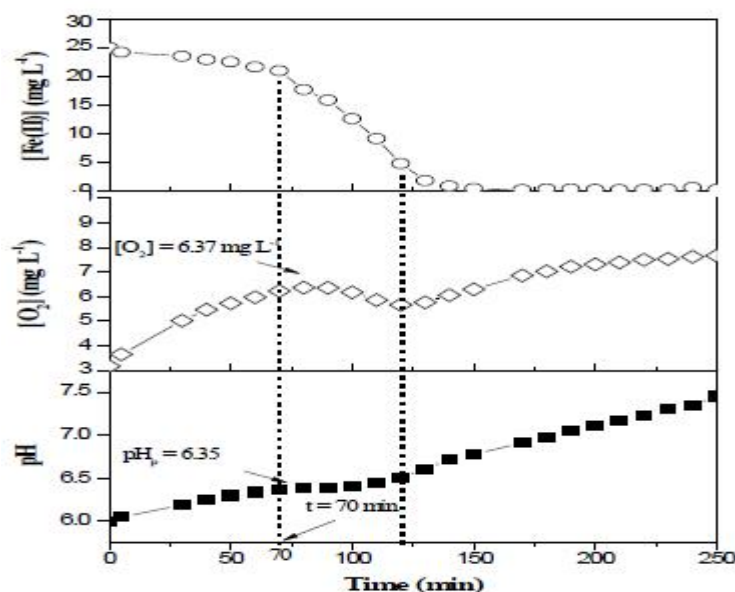


**Figure 2:** Variation of pH, dissolved oxygen concentration and total iron concentration vs. time : [Fe(II)]<sub>0</sub> = 25 mg/L, [HCO<sub>3</sub><sup>-</sup>] = 8 mM, pHi = 6 and T = 30°C.

At t=70 min, pH was reached a critical value of 6.35, noted precipitation pH (pHp), dissolved oxygen concentration was reached a level of 6.37 mg/L and [Fe(II)] was started dropping. After t = 70 minutes the pH was reached a steady state from 70 to 100 min (figure 2). The dissolved oxygen concentration was decreased from 6.37 to 5.65 mg/L announcing the end of the precipitation. The increase of pH is due to the competition between precipitation and CO<sub>2</sub> release, when the release of CO<sub>2</sub> prevails over precipitation. The Fe(II) concentration dropped drastically from 21 mg/L to 0.01 mg.L<sup>-1</sup> (figure 2) and the obtained precipitates were yellowish brown. These observations suggest

that, two iron precipitation states seem to exist: (i) a slow initial precipitation rate up to t = 70 min interpreted as the nucleation step followed by (ii) a high precipitation rate: the crystallite growth step, beyond t = 70 min.

### Effect of pH

To study the effect of pHi we performed 7 tests at different pHi: 6, 6.2, 6.4, 6.6, 6.8, 7 and 8 [HCO<sub>3</sub><sup>-</sup>] = 8 mM, [Fe(II)]<sub>0</sub> = 25 mg/L and at a temperature of 30°C. The results are shown in Figure 3 and table 1.

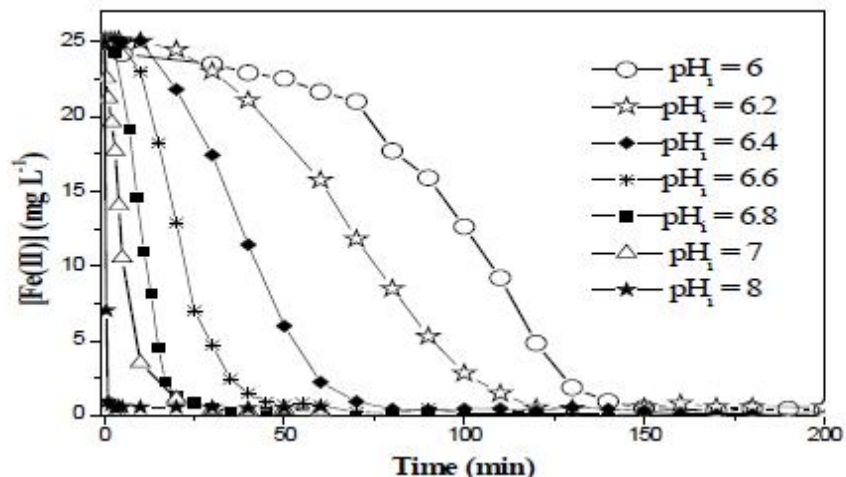


Figure 3: Variation of total iron concentration vs. time at different pHi;  $[HCO_3^-] = 8 \text{ mM}$  and  $T = 30 \text{ }^\circ\text{C}$ .

Figure 3 illustrates the evolution curves of the Fe(II) concentration as a function of time at different pHi. The results have shown that the higher the pHi was increased, the higher the concentration of Fe(II) was decreased. At pHi 7 and 8, Fe(II) concentration was dropped instantaneously and was reached zero value at the end of precipitation test in a few second.

With the pHi increasing, the nucleation precipitation step was faster due to the instantaneous precipitation giving small germination time (table 1). At pHi 8, nucleation step was so faster due to the high Fe(II) oxidation rate.

**Table 1.** Effect of pHi on  $t_b$ ,  $pH_p$  and precipitation ratio ( $\rho_p$ ) for  $[HCO_3^-] = 8 \text{ mM}$  and  $T = 30^\circ\text{C}$ .

pHi	6	6.2	6.4	6.6	6.8	7	8
$t_b$	70	50	32	15	8	3	--
$pH_p$	6.35	6.35	6.42	6.45	6.6	6.7	7
$\rho_p$ (%)	100	100	100	100	100	100	100

Similar results are found by (Davison et al., 1992)<sup>33</sup>. They find that, for an initial pH 8, 7, 6 and 5 at  $10^\circ\text{C}$ , the half-lives for the removal of Fe (II) are 2.34 min, 234 min, 390 h and 1625 days, respectively.

At high pH, the  $Fe(OH)_3$  precipitates easily<sup>34</sup>. Similar discussions are observed by other authors<sup>13,35,36</sup>. According to (Zhang et al., 1993)<sup>37</sup>, the affinity of  $Fe(OH)_3$  hydroxide surface for Fe(II) is higher at higher pH value. For pH = 8, the precipitation ratio  $\rho_p$  (%), determined from equation (9), achieved 100 % in few seconds. It is noteworthy that, for any pHi value, the precipitation is total,  $\rho_p = 100 \%$ .

Where,  $[Fe]_0$  is the iron concentration at  $t = 0 \text{ min}$  and  $[Fe]_t$  is the iron concentration at the end of precipitation test.

### Effect of bicarbonate concentration

To study the effect of bicarbonate concentration 4 tests at different bicarbonate concentration: 1 mM, 2 mM, 4 mM and 8 mM; pHi = 6;  $[Fe(II)]_0 = 25 \text{ mg/L}$  and  $T = 30 \text{ }^\circ\text{C}$  were performed. The results are shown in Figure 4 and table 2.

$$\dagger_p = \frac{[Fe]_0 - [Fe]_t}{[Fe]_0} \times 100 \quad (9)$$

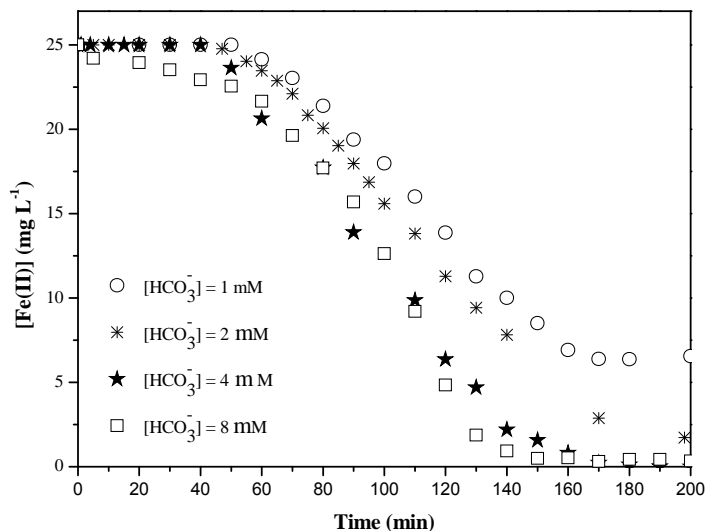


**Figure 4:** Variation of total iron concentration vs. time at different bicarbonate concentration for  $\text{pHi} = 6$  and  $T = 30^\circ \text{C}$ .

For  $\text{HCO}_3^-$  concentration of 1 mM, 2 mM and 4 mM the nucleation time ( $t_b$ ) was decreased when  $\text{HCO}_3^-$  concentration was increased (figure 4). For example,  $t_b$  was passed from 61 to 48 min when  $\text{HCO}_3^-$  concentration was increased from 1 to 4 mM, respectively (table 2). For  $\text{HCO}_3^-$  concentration of

8 mM,  $\text{Fe}(\text{OH})_3$  precipitation was instantaneously showing a great effect of bicarbonate ions concentration on the precipitation ratio, which was increased proportionally with  $\text{HCO}_3^-$  concentration. It was passed from 74.8 % to 100 % for  $\text{HCO}_3^-$  concentration 1 mM and 8 mM, respectively.

**Table 2.** Effect of bicarbonate concentration on  $t_b$ ,  $\text{pH}_p$  and precipitation ratio ( $\rho_p$ ) for  $\text{pHi} = 6$  and  $T = 30^\circ \text{C}$ .

$[\text{HCO}_3^-]$ (mM)	1	2	4	8
$t_b$	61	59	48	70
$\text{pH}_b$	6.2	6.1	6.1	6.35
$\rho_p$ (%)	74.8	90	100	100

This observed effect of bicarbonate can be explained by considering a combination of two factors: (a) the buffering capacity of bicarbonate ions, and (b) the effect of iron (II)-bicarbonate complexes on  $\text{Fe}(\text{OH})_3$  solubility.

In fact, for low bicarbonate concentrations (1, 2 and 4 mM) and the  $\text{CO}_2$  removal from solution by efficient aeration, the pH rise was not high enough to insure rapid and complete oxidation. Figure 5 shows pH

evolution for different  $\text{HCO}_3^-$  concentrations. During nucleation period, pH gradually was raised and was reached the value of 6.1 at  $t_b = 61$  min, however, no precipitation was occurred. During crystallization step, the solution has not sufficient buffering capacity to maintain steady the pH value, thus  $\text{Fe}(\text{OH})_3$  precipitation was caused a fall in pH values due to the releasing of  $\text{H}^+$  ions (reaction 3) (figure 4). There was no complete precipitation reaction when the concentrations of bicarbonate were 1 and 4 mM.

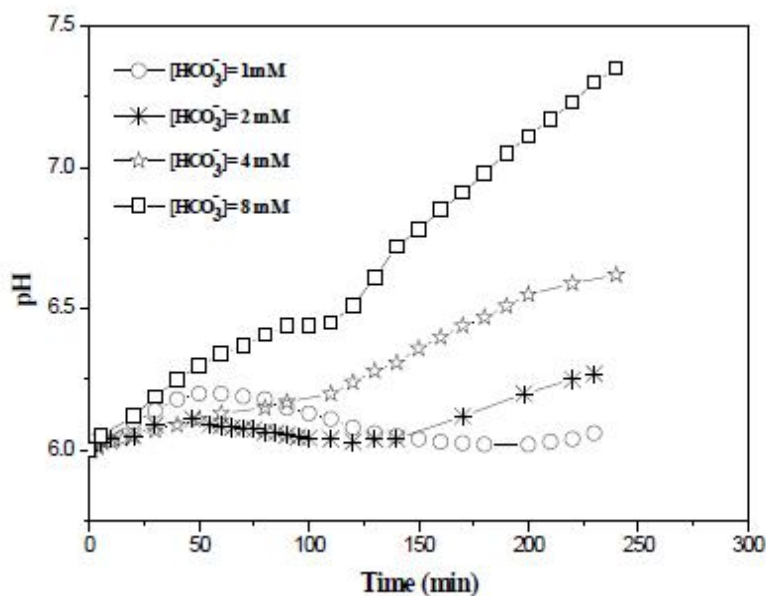


**Figure 5:** Variation of pH vs. time at different bicarbonate concentration for  $pH_i = 6$  and  $T = 30\text{ }^\circ\text{C}$ .

However, for the high bicarbonate concentration of 8 mM, the pH was increased, was reached the value 6.35 (figure 5) and then was remained constant during iron precipitation at a relatively high pH level due to the buffering effect of  $\text{HCO}_3^-$ . (Millero et al., 1995)<sup>14</sup> investigated the oxidation of Fe(II) by  $\text{O}_2$ . They find that, at pH of natural water, the  $(\text{Fe}(\text{CO}_3)_2)^{2-}$  and  $\text{Fe}(\text{CO}_3)(\text{OH})^-$  species are expected to be the main species involved in Fe(II) oxidation in bicarbonate solutions.

### Effect of temperature

To study the effect of temperature 4 tests at different temperature: 20, 30, 40 and 60°C;  $pH_i = 6$ ;  $[\text{Fe}(\text{II})]_0 = 25\text{ mg/L}$  and  $[\text{HCO}_3^-] = 8\text{ mM}$  were performed. The results are shown in Figure 6 and table 3.

The nucleation time  $t_b$  is five times lower at 40 °C than at 20°C. At the highest temperature 60°C, the nucleation step is not distinguished, the precipitation was instantaneously.

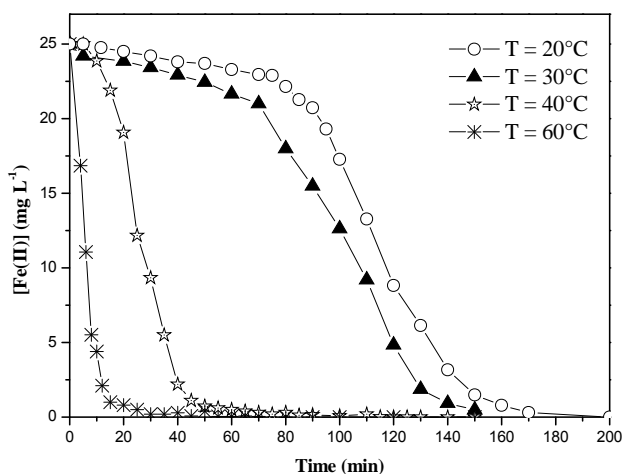


**Figure 6:** Variation of total iron concentration vs. time at different temperature for  $pH_i = 6$  and  $[\text{HCO}_3^-] = 8\text{ mM}$ .

The enhancement of iron precipitation can be attributed to the low solubility of iron hydroxide at high temperature. Other authors suggest that CO<sub>2</sub> release increases with the increasing of temperature, enhancing iron precipitation according to reaction (1)<sup>38</sup>. We can conclude that the increasing of temperature favors iron (III) precipitation despite the low precipitation pH value (pH<sub>p</sub>). (G. Montes-

Hernandez et al., 2011)<sup>39</sup> are studied the mechanism of goethite precipitation. They show that the kinetic behavior depends on the reaction temperature. Globally the nucleation-growth of goethite at 70 °C is close to three times faster than that at 30 °C. They also find that goethite is produced after 7 h of reaction at 70 °C, contrary after 24 h at 30 °C.

**Table 3.** Effect of temperature on t<sub>b</sub>, pH<sub>p</sub> and precipitation ratio (ρ<sub>p</sub>) for pHi = 6; [HCO<sub>3</sub><sup>-</sup>] = 8 mM.

T (°C)	20	30	40	60
t <sub>b</sub>	84	70	15	--
pH <sub>p</sub>	6.32	6.35	6.18	6.1
ρ <sub>p</sub> (%)	100	100	100	100

### Fe(OH)<sub>3</sub> precipitates characterization

The XRD patterns of Fe(OH)<sub>3</sub> precipitate formed at different pHi, different bicarbonate concentration and different temperature are shown in figure 7.

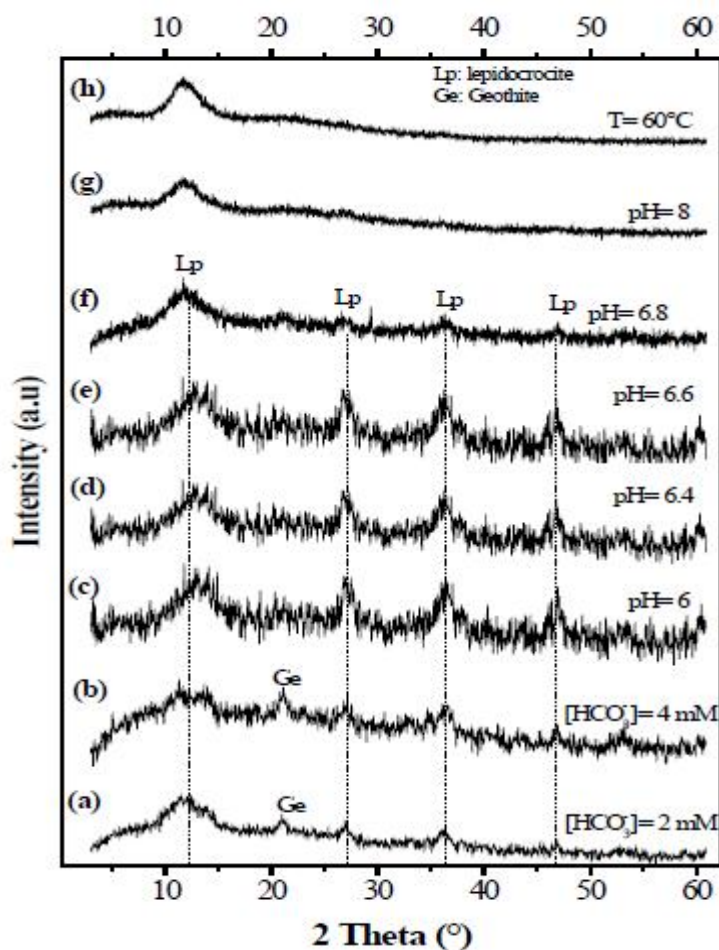


**Figure 7:** XRD patterns of iron (III) precipitates formed: (a), (b) and (c) at various bicarbonate concentration for pHi 6 and at 30°C, (c), (d), (e), (f) and (g) at various initial pH for [HCO<sub>3</sub><sup>-</sup>] = 8 mM and at 30°C, (c) and (h) at various temperature for pHi 6 and [HCO<sub>3</sub><sup>-</sup>] = 8 mM.

For precipitates formed at the range of pHi 6, 6.4, 6.6 and 6.8, the XRD patterns show broad peaks situated at d-spacings of 3.31, 2.49, 1.93 and 1.53 Å. These broad peaks are characteristic of lepidocrocite ( $-\text{FeOOH}$ )<sup>13,27,33</sup>. To the low bicarbonate concentrations, in addition to the characteristic peaks of lepidocrocite, another peak has been observed. It's situated at d-spacing of 4.1 Å, characteristic of goethite ( $-\text{FeOOH}$ ). XRD analysis has shown that the  $\text{Fe}(\text{OH})_3$  precipitates, later were crystallized to a more stable phase, lepidocrocite<sup>32,33</sup>. The crystallinity of lepidocrocite was reduced with an increase in pHi. Indeed, when the pHi was increased, the intensities of the above mentioned characteristic peak was

decreased and was disappeared completely at the highest pHi (pHi=8). Further, when temperature was increased to 60 °C, the mentioned characteristic peak disappeared. The XRD patterns indicate the formation of poorly-crystalline phase, associated to ferrihydrite. This form is known to be poorly crystalline and has a small particle size<sup>30</sup>. Nevertheless, pH and temperature are two parameters capable both to determine the supersaturation and than the stability of the species precipitated<sup>30,40,41,42</sup>. It was shown that iron ion is precipitated as goethite ( $-\text{FeOOH}$ ) from mild alkaline water and as ferric hydroxide (ferrihydrite,  $\text{Fe}(\text{OH})_3$ ) from highly alkaline water<sup>43</sup>.

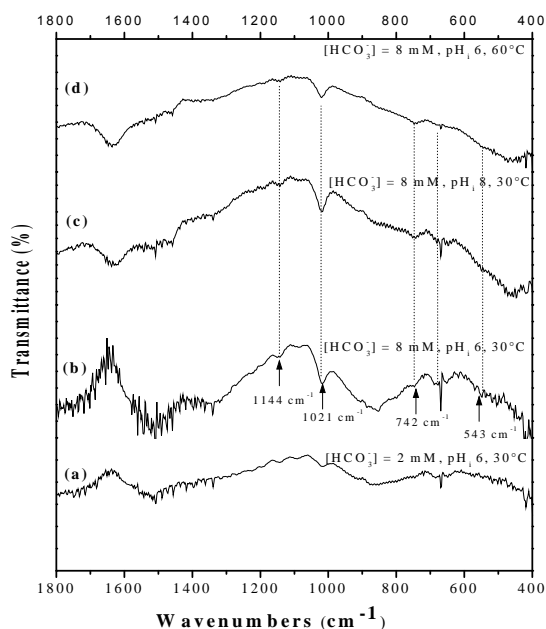


**Figure 8:** IR spectrum of the precipitate formed: (a) and (b) at various bicarbonate concentration for pHi 6 and at 30°C, (c) at pHi = 8 for  $[\text{HCO}_3^-] = 8 \text{ mM}$  and at 30°C, (d) at 60°C for pHi 6 and  $[\text{HCO}_3^-] = 8 \text{ mM}$ .

Figure 8 reports the FTIR spectra of precipitates obtained at pHi 6 and 8 (figure 8 b and c), bicarbonate concentration 2 and 8 mM (figure 8 a and b) and at temperature of 30 and 60 °C (figure 8 b and d). Like XRD diffraction results, the FTIR spectra was indicated the formation of lepidocrocite, characterized by its typical IR bands at 1144, 1021, 742 and 543  $\text{cm}^{-1}$ <sup>44,45</sup>. For the precipitate formed at the highest pH or the highest temperature (figure 8 c and d), the absorption band of lepidocrocite was observed. The FTIR analysis shows that lepidocrocite can be formed in any case of previous mentioned experimental condition of pH and temperature. The above results suggest that the  $\text{Fe}(\text{OH})_3$  precipitation by aeration leads to the formation of lepidocrocite particles.

## CONCLUSION

From the present results, we can conclude as follows:

1. Precipitation method by oxidation with air is appropriate for the removal of iron from synthetic solutions.
2. Precipitation is strongly dependent on pHi. Precipitation occurs in a few minutes at pHi 7 and 8, contrary at pHi 6 where precipitation occurs after one hour.
3. Because of the buffering effects of bicarbonate, in high bicarbonate concentration, massive iron precipitation is observed by air oxidation-precipitation method.

4. Because of the releasing of dissolved CO<sub>2</sub> in the solution when temperature increases, a massive precipitation of iron is observed.
5. The X-ray diffraction patterns of the Fe(OH)<sub>3</sub> precipitates shown that lepidocrocite was obtained during precipitation by aeration method. This observation was confirmed by IR spectra.
6. The pH and the temperature are two parameters capable to promote the formation of poorly crystalline iron oxyhydroxide which was close to the ferrihydrite.

## ACKNOWLEDGMENTS

The authors thank especially to the Laboratoire de Traitement des Eaux Naturelles, Technopole de Borj Cedria, Tunisie for recording FTIR and DRX.


## CONFLICTS OF INTERESTS

The authors declare that they have no conflict of interest.

## REFERENCES

1. D. Ellis, C. Bouchard, G. Lantagne, *Desalination*, **2000**, 130, 255–264.
2. A. J. Martín, *PhD thesis*, **2007**, Cranfield Univ. Uganda.
3. WHO, *Guidelines for Drinking Water Quality*, **2004**, 3<sup>rd</sup> ed., World Health Organization, Geneva, Switzerland.
4. S.K. Sharma, J. Kappelhof, M. Groenendijk, J.C. Schippers, *J. Water Supply Res. Technol.* **2001**, 50, 187–198.
5. M. Dekker, *B. Perekh (Ed.)*, **1988**, New York, NY (1988).
6. J. A. Salvato, *John Wiley and Sons*, **1992**, 4th Ed.
7. B. Morgan, O. Lahav, *Chemosphere*, **2007**, 68, 2080–2084.
8. W. Stumm, G.F. Lee, *Ind. Eng. Chem.* **1961**, 53, 143–146.
9. H. Tamura, K. Goto, M. Nagayama, *J. Inorg. Nucl. Chem.* **1976**, 38, 113–117.
10. M.M. Ghost, *Ann Arbor Sci. Publ.* **1974**, 5, 193–217.
11. W. Davison, G. Seed, *Geochim. Cosmochim. Acta*, **1983**, 47, 67–79.
12. W. Sung, J. J. Morgan, *Environ. Sci. Technol.*, **1980**, 14, 561–568.
13. F. J. Millero, S. Sotolongo, M. Izaguirre, *Geochim. Cosmochim. Acta*, **1987**, 51, 793–801.
14. D. W. King, H. A. Lounsbury, F. J. Millero, *Environ. Sci. Technol.*, **1995**, 29, 818–824.
15. T. Grundl, J. Delwiche, *J. Contam. Hydrol.* **1993**, 14, 71–97.
16. M. Henry, J.P. Jolivet, J. Livage, *Struct. Bond.*, **1992**, 77, 153–206.
17. F. Millero, *Geochimica et Cosmochimica Acta*, **1985**, 49, 547–553.
18. R. G. Wilkins, *Ilyn and Bacon*, **1974**, 403.
19. C.F. Beas Jr., R. E. Mesmer, *Wiley*, New York, **1976**, 489.
20. J. M. Longley, *MS Thesis*, **1961**, Dept. of Civ. Eng., Univ. of Illinois.
21. M. M. Ghosh, *San. Eng. Ser. No. 12.*, **1962**, Univ. of Illinois.
22. F.J. Millero, M. Izaguirre, V.K. Sharma, *Mar. Chem.*, **1990**, 22, 179–191.
23. F.J. Millero, M. Izaguirre, *J. Solution Chem.* **1989**, 18, 585–599.
24. J.O. Claassen, R.F. Sandenbergh, *Hydrometallurgy*, **2007**, 86, 178–190.
25. R. M. Cornell, U. Schwertmann, *Wiley VCH*, **1996**, Weinheim, New York.
26. U. Schwertmann, P. Cambier, E. Murad, *Clays Clay Miner*, **1985**, 33, 369–378.
27. J.A. Dirksen, T.A. Ring, *Chem. Eng. Sci.*, **1991**, 46, 2389–2427.
28. U. Schwertmann, R.M. Cornell, *Wiley-VCH, N.Y.*, **2000**, (2nd ed.)
29. A.C. Scheinost, U. Schwertmann, *Soil Sci. Soc. Am. J.*, **1999**, 63, 1463.
30. T. Misawa, K. Hashimoto, S. Shimodaira, *Corrosion Sci.*, **1974**, 14, 131–149.
31. U. Schwertmann, H. Fechter, *Clay Miner.*, **1994**, 29, 87–92.
32. X. Y. Gu, P.H. Hsu, *Soil Sci. Soc. Am. J.*, **1987**, 51, 469.
33. W. Davison, R.R. De Vitre, *Environmental particles. Lewis*, **1992**, In: J. Buffle & H. P. Van Leuwen (Eds), 315–355.
34. A. Alicilar, G. Meriç, F. Akkurt, O. endil, *J. Int. Environ. App. & Sci.*, **2008**, 3, 409–414.
35. S.P. Burke, S.A. Banwart, *Appl. Geochem.*, **2002**, 17, 431–443.
36. M. Hafsi, *Desalination*, **2001**, 134, 93–104.
37. Y. Zhang, L. Charlet, P. W. Schindler, *Colloids Surf.*, **1992**, 63, 259–268.
38. J. W. Morse, S. He, *Marine Chemisto*, **1993**, 41, 291–297.
39. G. Montes-Hernandez, P. Beck, F. Renard, E. Quirico, B. Lanson, R. Chiriach, N. Findling, *Cryst. Growth*, **2011**, 11, 2264–2272.
40. R.C. Mackenzie, R. Meldau, *Mineral Mag. London*, **1959**, 32, 153–165.
41. U. Schwertmann, *Z. Pflanz. Boden.* **1965**, 108, 37–45.
42. E. Murad, U. Schwertmann, *Clays Clay Miner.* **1983**, 31, 277–284.

43. R.M. Cornell, U. Schwertmann, *VCH New York*,  
**1996**.
44. U. Schwertmann, R.M. Cornell, *VCH Publishers*,  
**1991**, Inc. Weinheim, Germany.
45. J. D. Russell, A. R. Fraser, *J. Wilson Ed.*  
(*Chapman and Hall, London*), **1994**, Chap. 2.

Access this Article in Online	
	Website: <a href="http://www.ijcrcps.com">www.ijcrcps.com</a>
	Subject: <a href="#">Chemistry</a>
Quick Response Code	
DOI: <a href="https://doi.org/10.22192/ijcrcps.2019.06.12.001">10.22192/ijcrcps.2019.06.12.001</a>	

How to cite this article:

Wided Mejri, Abdou Salam Manzola, Mohamed Tili and Mohamed Ben Amor. (2019). Study of iron (III) hydroxide precipitation in bicarbonate aqueous solutions. *Int. J. Curr. Res. Chem. Pharm. Sci.* 6(12): 1-11.  
DOI: <http://dx.doi.org/10.22192/ijcrcps.2019.06.12.001>